Electronic Spectra and an Angular-Overlap-Model Analysis of *trans*-$[Cr(ox)_2(py)_2]^-$

Thomas Schönherr and Joachim Degen

Institut für Theoretische Chemie, Heinrich-Heine-Universität Düsseldorf, Düsseldorf

Z. Naturforsch. **45a**, 161–168 (1990); received October 10, 1989

Dedicated to Prof. Dr. H.-H. Schmidtke on the occasion of his 60th birthday

The quartet and doublet transition in *trans*-$[Cr(ox)_2(py)_2]^-$ show considerable band splittings due to the low-symmetry of the ligand field. The components of $^2E_g(O_h)$ and $^2T_{1g}(O_h)$ have been assigned by analysis of vibrational sideband structures in the low-temperature absorption and emission spectra. The energy level scheme has been rationalized in terms of the angular-overlap model. The different contributions of π bonding from the oxalate (π donor) and pyridine (π acceptor) ligands give an explanation of the uncommon quartet band splittings. The doublet energies depend strongly on the molecular geometry. In particular, a reduction of the oxalate bite angle to about 84° has been derived from the spectral band fit.

Key words: Angular-overlap model, Chromium(III) complexes, Vibronic spectra, Spectrum-structure correlations.

Introduction

Experimental and theoretical investigations on the optical spectra of chromium(III) complexes have become a renascent field of research activity mainly for the following reasons: (i) Intraconfigurational transitions within the t_{2g} subshell yield detailed sharp-line spectra (doublet bands) which often are highly resolved at low temperatures; (ii) a great variety of chromium complexes (homoleptic and mixed ligand complexes) is already known, allowing for investigations within a series of similar compounds; (iii) Cr^{3+} doped materials (minerals, glass ceramics) are of current interest for possible applications in tunable solid state lasers [1] or as solar energy concentrators [2].

The d-electron energy level scheme of Cr(III) complexes can generally be successfully described by an electrostatic perturbation on the Cr^{3+} multiplets within the framework of the semiempirical ligand field approach [3]. In recent years increasing attention has been paid to the angular-overlap-model (AOM), which is based on the additivity of metal-ligand interactions using antibonding parameters of σ and π type [4–8]. The advantage of the AOM over the conventional ligand field theorey (LFT) arises from the local parametrization in this model, in which the electrostatic potential can be easily expressed for any geometry of the chromophore [7]. Furthermore, AOM parameters have been found to be transferable to some extent and can be used for predictions concerning spectra and structures of related complexes. Chelated transition metal complexes provide suitable examples for investigating the specific influence of the molecular structure on the d-electron states. Especially, strong π bonding interactions can give rise to considerable band splittings in the electronic spectra, in particular, if ligands such as oxalate (ox^{2-}), acetylacetonate ($acac^-$) or 2,2′-bipyridine (bpy) are involved [6, 8]. Since this model can explain the d–d spectra of such tris-chelated compounds, it should be also applicable for predictions to similar complexes.

The present work deals with the optical absorption and emission spectra of *trans*-{bis(pyridine)-bis(oxalato)}chromate(III), where strong π interactions are expected due to the low-lying π MO's of the pyridine and oxalate ligators. Zero-phonon lines due to the spin-forbidden transitions are investigated by analyzing the highly resolved vibrational sideband structures in comparison with infrared data. We have further addressed the question of how π bonding, at the actual geometric positions of the ligands, influences the sign and the magnitude of the doublet splittings. These are by far more informative about small structural changes than the broad quartet bands due to the spin-allowed transitions.

Reprint requests to Dr. Th. Schönherr, Institut für Theoretische Chemie, Universität Düsseldorf, Universitätsstraße 1, D-4000 Düsseldorf 1.

0932-0784 / 90 / 0200-0161 $ 01.30/0. – Please order a reprint rather than making your own copy.

In a previous investigation, using Xα-scattered wave SCF calculations Wheeler and Poshusta have suggested unusual large quartet band splittings [9]. According to the lowest d-electron configuration the electronic ground state was found to be a $^4B_{1g}$. The calculated SCF energies of d–d transitions were explicitly claimed to be in good agreement with the UV/VIS absorption spectrum, however, the given spectral assignments for the higher quartet states differ distinctly from those given for similar complexes [3], and, furthermore, they are at variance with the predictions of the ligand field approach.

Experimental

The potassium salt of *trans*-$[Cr(ox)_2(py)_2]^-$ was prepared from *trans*-$K[Cr(ox)_2(H_2O)_2] \cdot 3\,H_2O$ as described previously [10]. Recrystallization from aqueous solution was performed in the dark to prevent hydrolysis reactions. The compound precipitated as pink crystalline needles. An elementary analysis yielded the theoretical values. The isopentylammonium salt was obtained by metathesis of *trans*-$[Cr(ox)_2(py)_2]^-$ using saturated aqueous solutions of $K[Cr(ox)_2(py)_2]$ and $(H_3N-C_5H_{11})Cl$.

The room-temperature absorption spectrum was recorded with a Cary 17 spectrophotometer. High-resolution absorption (emission) spectra of crystalline powders were measured at helium temperatures using a McPherson 0.5 m double (Jobin Yvon 0.25 m) monochromator and red-sensitive GaAs photomultipliers. Temperatures down to 10 K were achieved with a helium bath-cryostat (CRYOVAC). Time-resolved emission spectra were obtained with a multichannel analyser system (EG & G).

The infrared spectrum in the 50–4000 cm^{-1} range was measured by the KBr pellet and polyethylene disc technique, respectively, with a Bruker 113 v vacuum Fourier spectrometer.

Results and Discussion

Spin-allowed Transitions

The room-temperature absorption spectra of 0.02 molar aqueous solutions of the potassium and isopentylammonium salts show a band pattern as typically found for octahedrally coordinated chromium(III) complexes in the visible/uv region with two broad quartet bands (Figure 1). The small molar extinction coefficients ($\varepsilon = 32(26)$ for the potassium (isopentylammonium) salt) reflect the presence of an inversion center in the molecule requiring a vibronic coupling mechanism which involves higher electronic states of *odd* parity for the Laporte forbidden d–d transitions. For a qualitative description of the spectra within the convenient ligand field approach the sym-

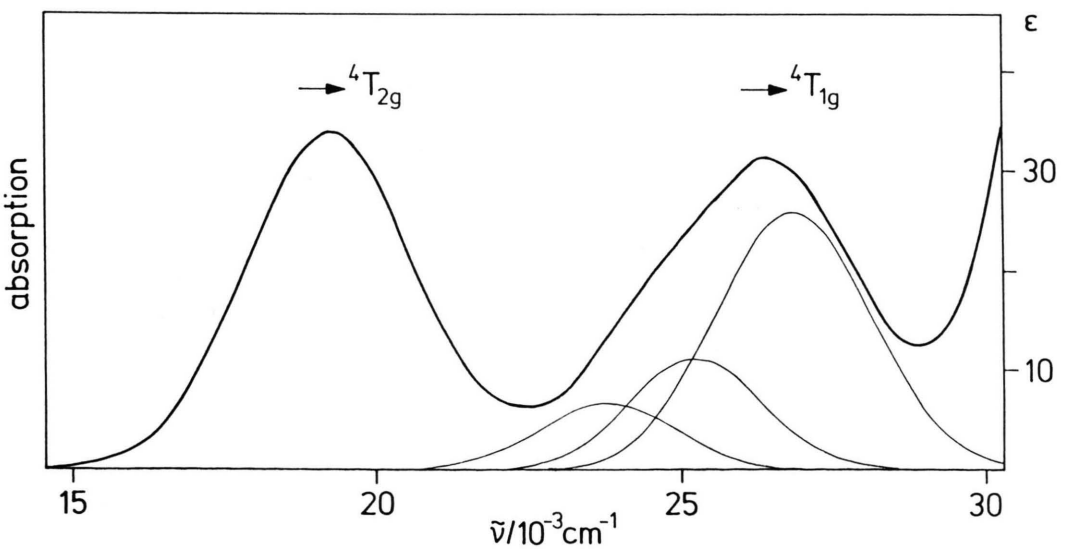

Fig. 1. Room temperature absorption spectrum of $K[Cr(ox)_2(py)_2] \cdot 2\,H_2O$. The given band deconvolution for the $^4A_{2g} \rightarrow {}^4T_{1g}(O_h)$ transition was performed by a least square fit using gaussian band shapes.

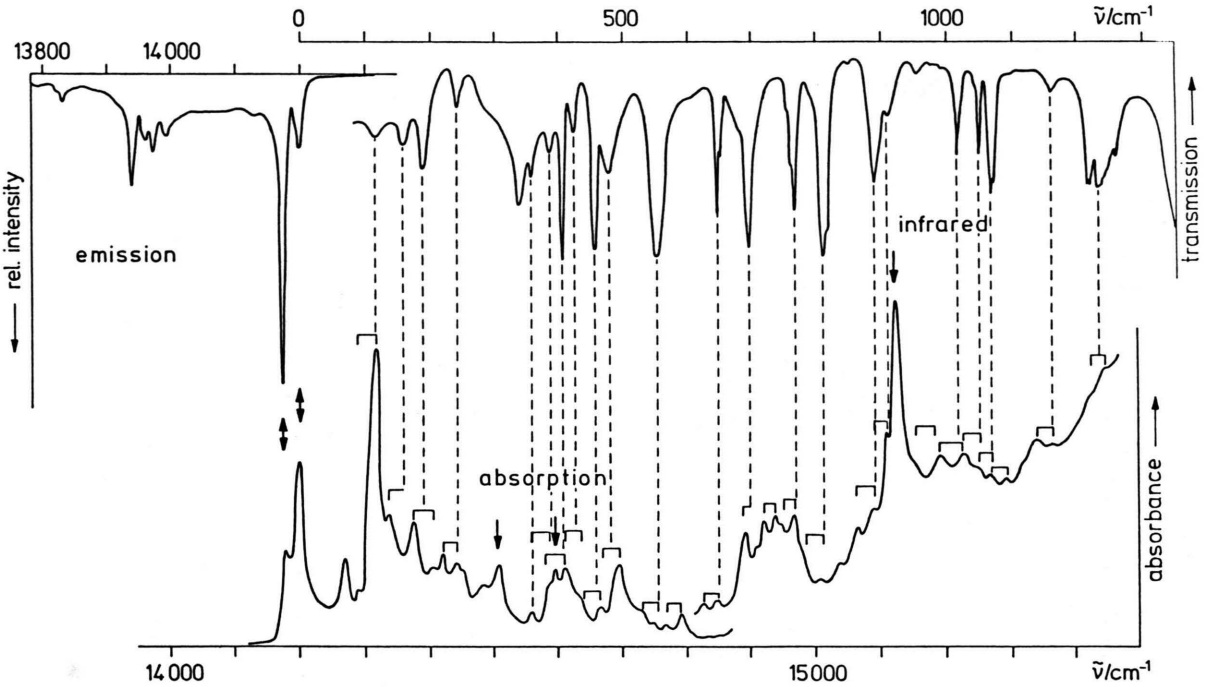

Fig. 2. Near-infrared absorption and the origin region of the 514 nm excited emission spectrum $K[Cr(ox)_2(py)_2] \cdot 2H_2O$ obtained at $T \approx 10$ K. The IR spectrum ($T \approx 295$ K) is correlated to vibrational sidebands of the $^4A_{2g}(O_h) \rightarrow {}^2E_g(O_h)$ transitions. Zero-phonon origins due to the spin-orbit levels of $^2T_{1g}(O_h)$ are indicated by arrows.

metry of the CrO_4N_2 chromophore can be approximated at D_{4h}. Then, considering only diagonal elements of the AOM perturbation matrices in the strong field approach [11] the band splittings of $^4T_{2g}(^4E-{}^4B_2)$ and $^4T_{1g}(^4E-{}^4A_2)$ are calculated to

$$\Delta E_{1/2} = 2\delta\pi \mp 3/2\,\delta\sigma$$

with the abbr.: $\delta\lambda = e_\lambda(ox) - e_\lambda(py)$; $\lambda = \sigma, \pi$. The parameters e_λ describe the interaction between a single ligator atom and the d-electron orbitals assuming rotational symmetry around the metal-ligand axis, where the label λ refers to the irreducible representations of the $C_{\infty v}$ group [5].

In general, the effect of σ antibonding mainly influences these level splittings, however, the significantly different π contributions of oxalate (π donor, $e_\pi > 0$) and pyridine (π acceptor, $e_\pi < 0$) leads here to $\delta\pi \approx \delta\sigma > 0$. Using AOM parameters as given by Schaeffer [5] and Atanasov et al. [6], one can expect splittings of about 500 cm^{-1} ($^4T_{2g}$) and 3000 cm^{-1} ($^4T_{1g}$) (*vide infra*). This is reflected in the spectrum by the broad shape of the higher quartet band. A deconvolution procedure (least squares fit) of the experimentally obtained band pattern yields maxima at 23 700, 25 200, and 26 800 cm^{-1}, respectively, for the split levels of $^4T_{1g}$. The appearance of three spectral maxima is caused by the actual molecular symmetry, which should be close to D_{2h}, where orbitally degenerate states cannot occur. For the low-energy spin-allowed transition $^4A_{2g} \rightarrow {}^4T_{2g}$ only a slightly unsymmetrical bandshape is observed. In this case the determination of the expected three split levels is not possible because of the broadness of the quartet bands preventing the identification of transitions separated by less then ≈ 1000 cm^{-1}.

Spin-forbidden Transitions

The intercombination band region was measured on microcrystalline powders at helium temperatures. Spectra of the potassium salt are given in Fig. 2, showing a detailed vibrational fine structure both in absorption and emission. The $^2E_g(O_h)$ origins, which are separated by 24 cm^{-1}, are located with the medium strong bands at 14176 and 14200 cm^{-1} at the low energy end of the absorption spectrum. Provided both

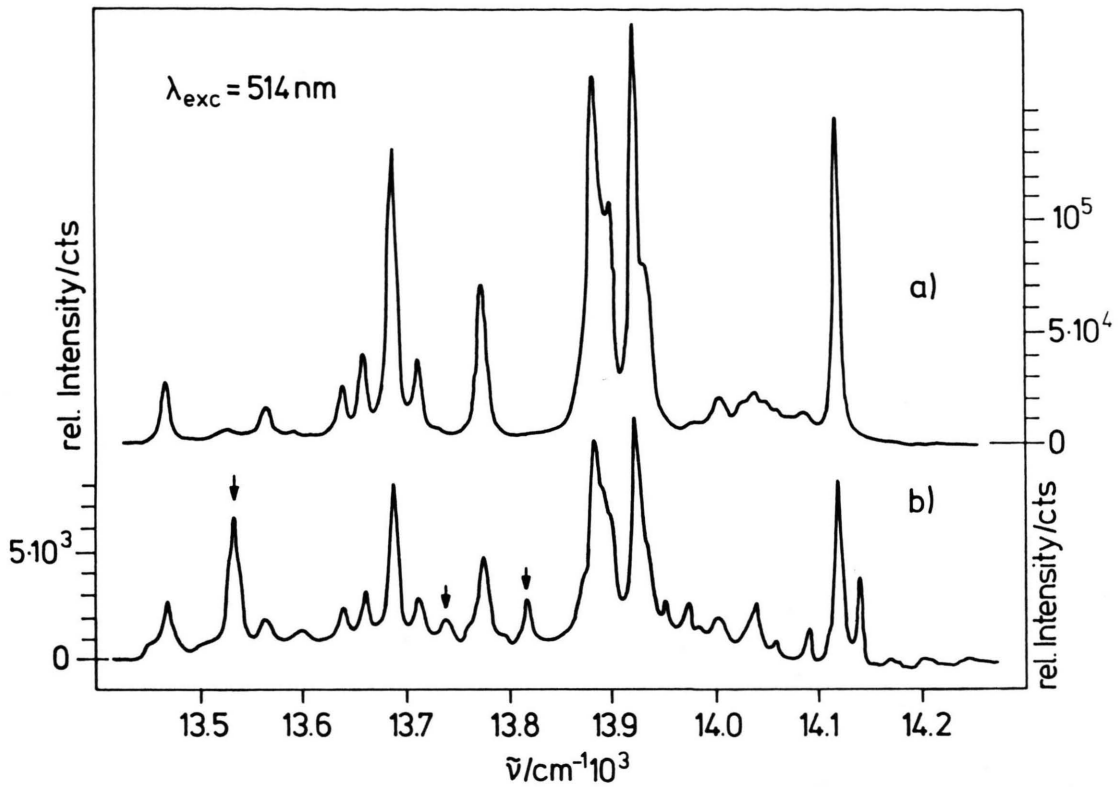

Fig. 3. Emission spectra of $(C_5H_{11}NH_3)[Cr(ox)_2(py)_2]$ measured at $T \approx 10$ K: a) total intensity; b) obtained after a delay time of 13 ms.

split components of $^2E_g(O_h)$ are not in thermal equilibrium because of negligible phonon coupling, this assignment is supported by the emission spectrum supplying a corresponding pair of lines at these wavenumbers. Alternatively, the transition into the higher split component of $^2E_g(O_h)$ could be identified to the medium strong band at 14 270 cm^{-1} in better agreement with the calculated $^2E_g(O_h)$ splitting (cf. *next section*). This assignment would, however, require the existence of two nonequivalent chromium sites in the crystal lattice of the potassium salt in order to obtain a reasonable interpretation of the complete vibrational finestructure (*vide infra*). For other salts of the present complex different spectral features with respect to the number of independent chromium sites are expected. Therefore, we have measured the absorption spectrum of $(H_3N{-}C_5H_{11})[Cr(ox)_2(py)_2]$ containing the much larger isopentylammonium anion. From a careful analysis of this spectrum we determined the energy splitting of the lowest zero-phonon lines to be 25 cm^{-1}, i.e. almost the same as for the potassium salt. The only remarkable difference between the doublet spectra of these salts was observed in the lower intensity of the zero-phonon lines (compared to the vibronic sidebands) for the isopentylammonium salt which indicates a slightly higher deviation from inversion symmetry in the potassium salt.

Additional support for the identification of these electronic origins comes from a time resolved luminescene study. For the isopentylammonium salt lifetimes were measured to $\tau = 10$ ms ($\tau = 25$ ms) for the long (short) wavelength component, respectively. From that significant different emission spectra can be expected when various delay times were chosen. This is illustrated in Fig. 3, where the steady-state spectrum is given (a) together with the emission bands obtained after a delay time of 13 ms (b). Bands due to the short wavelength component (larger τ) are considerably increased in the delayed spectrum, especially the zero-phonon line and the vibronic sidebands at 13 817, 13 739, and 13 532 cm^{-1}, which are indicated by arrows in Figure 3 b. The relative intensities of vibronic

sidebands corresponding to these origins should be similar when caused by two different sites. The delayed spectrum, however, did not show a doubling of the vibronic structure giving further support for the assignment of the two zero-phonon lines to different electronic states resulting from $^2E_g(O_h)$.

Towards higher energy the absorption spectrum can almost completely be interpreted in terms of vibrational structure (*promoting modes*) upon the $^2E_g(O_h)$ zero-phonon transitions which is illustrated in Fig. 2 by the correspondence between the absorption and infrared transitions. Again an alternative assignment of the higher split level of $^2E_g(O_h)$ is considered unlikely, primary reason being significantly less coincidences for corresponding vibrational sidebands. Table 1 compiles the data obtained from the vibronic analysis based on the 24 cm^{-1} splitting of $^2E_g(O_h)$ together with the relevant infrared frequencies of the complex. The majority of the vibronic sidebands yields vibrational energies which are evidently

Table 1. Vibrational intervals in the $^4A_{2g} \leftrightarrow {}^2E_g(O_h)$ spectra and corresponding infrared frequencies of $K[Cr(ox)_2(py)_2] \cdot 2\,H_2O$.

Absorption		Emission		Infrared	Assignments[a]
(14176)	(14200)	(14172)	(14198)		zero-phonon $^4A_{2g} \leftrightarrow {}^2E_g(O_h)$
	70		73		lattice
114	116	120	116	120	δ(O–Cr–O)
164		164		164	
199	204	205	210	(189)	σ(Cr–N): a_g^b
240	242	238	243	240	δ(O–Cr–O) + δ(O–Cr–N) + ring (ox)
315	308		304		
		346		346	
	359			356	
383	383	387	385	386	
407	413	408	413	408	
437	437	432	434	426	py-16
	466		465	459	ring (ox)
490	495	489	493	482	σ(Cr–O)
552	548	557		553	
588	593	589			$387 + \sigma(Cr-N)_{a_g}$
645	641	653	655	651	py-6
705		704	702	698	py-11
742	737	739	730		$557 + \sigma(Cr-N)_{a_g}$
777	766	770	765	768	py-4
790		793		810	δ(O–C=O)
882	883	885	873	890	py-5
907	903	904		912	σ(C–C)
980	990	976	991		$770 + \sigma(Cr-N)_{a_g}$
1014	1025	1021	1025	1016	py-1
1049	1050		1047	1049	py-12
1074	1069	1073		1072	py-18
1093	1089	1096	1099		$885 + \sigma(Cr-N)_{a_g}$

[a] Assignments of internal pyridine modes after [12].
[b] See text.

due to vibrations localized at the pyridine ligands as *promoting modes* mixing odd contributions into the concerned ligand field states of *even* parity. Besides the contributions of Cr–N displacements, one can derive assignments from the normal vibrations of the free pyridine in a one-to-one correspondence as have been given for a series of compounds with other transition metal ions [12]. It is noted that the vibrational interval $\sim 205\ cm^{-1}$, apart from the zero-phonon both in absorption and emission, is distinctly shifted to higher energy when compared to the intense infrared peak at 189 cm^{-1}, which we assign to the antisymmetric stretching mode $\sigma(Cr-N)_{as}$. However, since the interval of 205 cm^{-1} also appears in combination with other internal pyridine modes (cf. Table 1) this vibration is probably due to the totally symmetric σ(Cr–N) mode. The occurrence of an *accepting mode* of *even* parity gives rise to corresponding geometric displacements of the excited state potential surface relative to that of the ground state [13], which, likewise, has been observed in the vibronic spectra of other axially distorted chromium(III) complexes, e.g. *trans*-$[Cr(py)_4F_2]^+$ [14]. This strongly demonstrates the important role of metal-pyridine π bonding. Due to the acceptor property of the ligand some d-electron density is transferred into the pyridine ring when the lowest doublet states are excited. Because of the antibonding character of the metal t_{2g} orbitals, a reduction compression of the Cr–N bond length must be expected for the equilibrium geometry of the emitting state.

Only a few peaks could not be assigned by comparison of the data obtained from absorption, emission and infrared measurements. They can serve for the detection of the origins due to the higher $^2T_{1g}(O_h)$ state, which splits through the spin-orbit coupling and the low-symmetry ligand field into three Kramers doublets. The two medium intense peaks at 14 508 and 14 595 cm^{-1} and the relatively strong peak at 15 121 cm^{-1} differ from the $^2E_g(O_h)$ split levels by 332, 419, 945 cm^{-1} and 308, 395, 921 cm^{-1}, respectively. Since they have no correspondence in the emission nor infrared spectrum these peaks are reasonably assigned to zero-phonon lines. Based on these origins, some of the weaker vibronic sidebands defying an assignment upon $^2E_g(O_h)$ can be interpreted as transitions into $^2T_{1g}(O_h)$: especially vibrational energies of 168, 201, 325, and 405 cm^{-1} are observed, which support the given location of these electronic origins.

Both of the spin-orbit components resulting from the $^2E_g(D_{4h})$ split level are depressed by a large second-order coupling, which is proportional to $(\delta\pi)^2$ [13], and, on the other hand, all perturbation matrix elements $\langle {}^2\Gamma_g | V_{tet} | {}^2A_{2g} \rangle$ vanish for symmetry reasons when $^2\Gamma_g(D_{4h})$ represents any state with t_{2g} electron configuration (this is also true for D_{2h} symmetry!). Therefore, $^2A_{2g}(D_{4h})$ is almost unchanged on symmetry reduction and can be assigned to the peak at 15 121 cm^{-1}. The stabilization of the other two split levels is in accordance with the assignments proposed from the vibronic analysis of the intercombination region. Similar band splittings have been observed for other tetragonal chromium complexes, where significantly different π bonding in the xy and xz, yz planes is involved, e.g. for a series of halogonopentaamminechromium(III) salts [13] or for *trans*-$[Cr(py)_4F_2]^+$ [14]. The remarkably higher intensity of the $^4B_{1g}(D_{4h}) \rightarrow {}^2A_{2g}(D_{4h})$ transition relative to the other transitions into $^2T_{1g}(O_h)$ has been already observed in these complexes giving further confirmation of the present assignments.

Angular-overlap Calculations

In order to study the factors which influence the d-level splittings we have performed a series of calculations by diagonalizing the full 120×120 secular determinant which arises from the perturbated d^3 system [7]. Our calculations were based on the *additive* AOM which also accounts for the bidentate oxalate ligand [6], although orbital phase relations have to be considered in chelate complexes leading to *non-additive* contributions to the metal-ligand bond energy. π bonding was described by parallel and perpendicular contributions with respect to the orientation of the π systems of the ligands. For the pyridine ligand $e_{\pi\parallel}$ can be set to zero because of negligible contributions of the d-sp^2 interaction. For the oxalate ligand the parameter ratio $e_{\pi\parallel}/e_{\pi\perp}$ was chosen to 0.6 from reasonable values of the corresponding overlap integrals. Then, a total of seven electronic and two geometric parameters (*vide infra*) was included in the calculations, confronting us with the problem of overparameterization which may allow for a good fit even for incorrect assignments. The Racah parameters B and C, which represent two-electron repulsion integrals from the spherical treatment, insignificantly influence the low-symmetry level splittings considered here and can be obtained in good approximation from the quartet band separation ($\approx 12\,B$) and from the position of the lowest doublets ($\approx 9\,B + 3\,C$) without further variation. The doublet splittings, which are experimentally resolved in our spectra, depend to some extent on the value of the spin-orbit coupling parameter ζ. However, since qualitative aspects of the AOM results will be of more importance for the present investigation we fixed in all of our calculations this parameter to 200 cm^{-1}, which is in agreement with ζ values given for related complexes [6, 7, 13].

We started our calculations using values for e_σ and e_π as given in the literature [5, 6], since the AOM parameters should be transferable to a large extent. The geometry of the CrN_2O_4 entity was changed from an octahedron of D_{4h} symmetry (all angles around the metal were assumed to be 90°) to D_{2h} symmetry by varying the oxalate bite angle α. The latter should mainly be determined by the electronic structure of the isolated oxalate anion. In $Cr(ox)_3^{3-}$ salts it was found between 82° and 85° [15, 16]. As shown in Fig. 4, the calculated quartet splittings are in agreement with the experimental results (cf. Fig. 1) only when the value of the bite angle is in the expected range. The splitting of the ground state $^4A_{2g}$ is negligible small (< 1 cm^{-1}) and omitted in the Figure. An alternative assignment for the spin-allowed transitions, where the higher quartet band covers transitions into low-symmetry split components of $^4T_{2g}$ [9], could not be reproduced within reasonable upper and lower limits of the model parameters.

The influence of the bite angle on the doublet transitions is also depicted in Figure 4. Again, an α value of about 84° leads to a satisfying fit of the experimentally obtained splitting pattern of ^2E_g, $^2T_{1g}(O_h)$ giving additional support for our interpretation of the quartet bands. The results show, in fact, the validity of the AOM approach, which has immediately (i.e. without any parameter fit procedure) yielded a reasonable description of the energy level scheme. It is noted that this clearly contradicts the calculated quartet energies obtained by the Xα-scattered wave method [9], demonstrating the problems of describing open-shell multiplets within an orbital approximation.

For a closer inspection of effects due to parameter variations we will discuss some calculations on the doublet states, which are determined more precisely by the spectroscopic experiments. Figure 5a gives an impression of the large influence of the π anisotropy of the oxalate on the doublet level scheme, where deviation from the expected $e_{\pi\parallel}/e_{\pi\perp}$ ratio leads to band

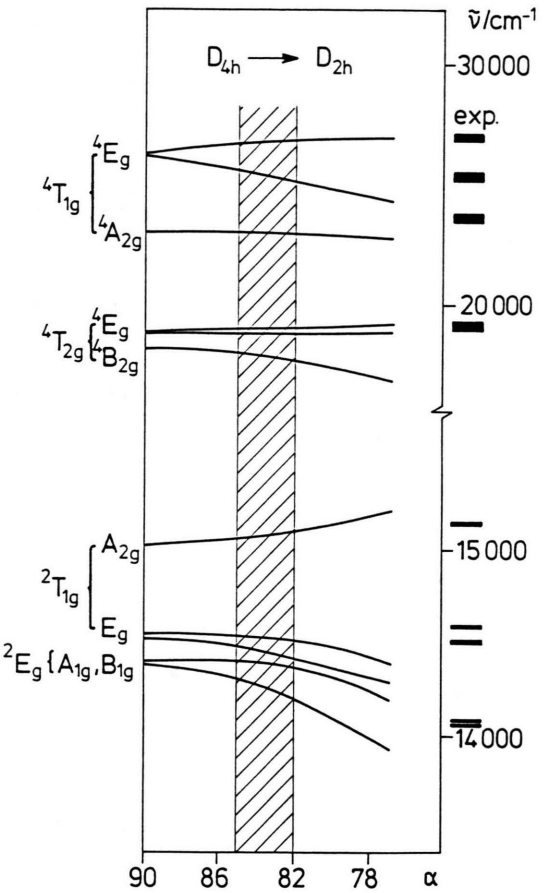

splittings far away from the experimental results. Due to the broadness of the spin-allowed bands, the band-shapes of the quartets are less influenced by that parameter variation which is not discussed here.

Finally, we will consider the contribution to the π bonding from the pyridine ligand. Low-lying LUMO's are responsible for the *acceptor* property ($e_{\pi\perp}(py) < 0$) which is visualized by the appearance of internal pyridine vibrations as promoting and accepting modes in the intercombination spectra (*vide supra*). In Fig. 5b the effect on the doublet level scheme is depicted for a wide variation of the axial π antibonding parameter. Again, the experimental results can be satisfactorily fitted within the expected range for $e_{\pi\perp}(py)$ between -500 and $-750\ cm^{-1}$. The fictive level sequence on the right side of the diagram reflects an almost octahedral effective ligand field according to similar σ and π contributions of axial and equatorial ligands.

It should be mentioned that the calculated separation of the $^2E_g(O_h)$ split levels is larger ($>40\ cm^{-1}$)

Fig. 4. Calculated energy splittings of excited d-states for deviations of the oxalate bite angle α. The AOM, electronic repulsion and spin-orbit parameters are (in cm^{-1}): $e_\sigma(py) = 5800$, $e_\sigma(ox) = 6750$, $e_{\pi\perp}(py) = -580$, $e_{\pi\parallel}(py) = 0$, $e_{\pi\perp}(ox) = 600$, $e_{\pi\parallel}/e_{\pi\perp}(ox) = 0.6$, $B = 650$, $C = 3200$, $\zeta = 200$. ▨: Expected region for α.

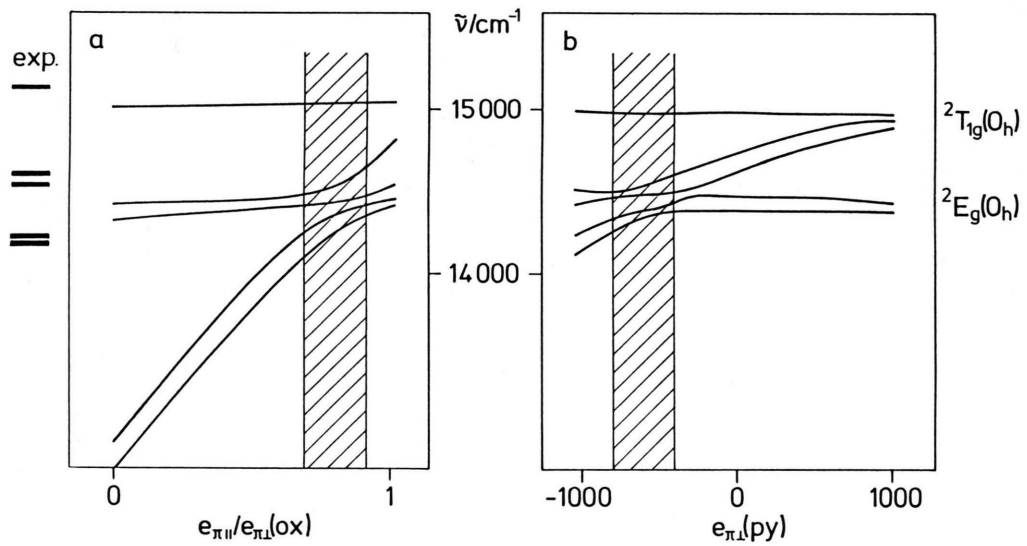

Fig. 5. Calculated doublet energies obtained from the anisotropy effect of the oxalate π bonding [a] and from the variation of the axial π contribution $e_{\pi\perp}(py)$ [b]. For the other parameter values see legend of Figure 4. ▨: Parameter region derived from a fit of the observed transitions.

than the observed value of 24 cm^{-1}. Another geometric parameter, the variation of the twist angle ψ, i.e. the orientation of the pyridine plane with respect to the x, y cartesian axes, influences the magnitude of the doublet splittings to some extent leading to a best fit for $\psi = 45°$. However, we could not reproduce the small $^2E_g(O_h)$ splitting when the relatively large ^2E_g–$^2T_{1g}(O_h)$ separation as well as the different shapes of the quartet bands were simultaneously considered. Other geometric effects are unlikely and not concerned here, since the assumption of an almost perfect D_{2h} symmetry for the chromophore is consistent with our results. Two reasons may be responsible for the inaccurate description of the $^2E_g(O_h)$ splitting: better results were obtained by Schmidtke et al. [13] for some tetragonal chromium(III) complexes when symmetry adapted π orbital expansion coefficients are introduced into the electron repulsion terms; on the other hand, the spin-orbit coupling parameter ζ, which was fixed to 200 cm^{-1} in all of our calculations, strongly influences the splittings of the lowest excited state, $^2E_g(O_h)$, and of the ground state $^4A_{2g}(O_h)$. The latter was claculated between 0.02 and 0.03 cm^{-1}, which could not be resolved in any of our spectra. Therefore, more precise calculations would require additional information from EPR or related techniques.

[1] B. Struve and G. Huber, Appl. Phys. **B 36,** 195 (1985).
[2] R. Reisfeld, Mater Sci. Eng. **71,** 375 (1985).
[3] A. B. P. Lever, Inorganic electronic spectroscopy, 2nd ed., Elsevier Science, Amsterdam 1984.
[4] C. K. Jørgensen, R. Pappalardo, and H.-H. Schmidtke, J. Chem. Phys. **39,** 1422 (1963).
[5] C. E. Schaeffer, Struct. and Bonding **5,** 68 (1968).
[6] M. Atanasov, T. Schönherr, and H.-H. Schmidtke, Theor. Chim. Acta **71,** 59 (1987).
[7] P. E. Hoggard, Coord. Chem. Rev. **70,** 85 (1986).
[8] A. Ceulemans, M. Dendooven, and L. G. Vanquickenborne, Inorg. Chem. **24,** 1153 (1987).
[9] W. D. Wheeler and R. D. Poshusta, Inorg. Chem. **24,** 3100 (1985).
[10] G. B. Kauffman and D. Faoro, Inorg. Synth. **17,** 147 (1977).
[11] P. E. Hoggard, Z. Naturforsch. **36a,** 1276 (1981).
[12] N. S. Gill, R. H., Nuttal, D. E. Scaiffe, and D. W. A. Sharp, J. Inorg. Nucl. Chem. **18,** 79 (1961).
[13] H.-H. Schmidtke, H. Adamsky, and T. Schönherr, Bull. Chem. Soc. Japan **61,** 59 (1988).
[14] C. D. Flint and A. P. Matthews, Inorg. Chem. **14,** 1008 (1975).
[15] J. N. Niekerk and F. R. L. van Schoening, Acta Cryst. **5,** 499 (1952).
[16] D. Taylor, Austr. J. Chem. **31,** 1455 (1978).